Journal of Cellular Biochemistry 83:532–546 (2001)

ARTICLES

# Biochemical and Morphogenic Effects of the Interaction Between Protein Kinase C-Epsilon and Actin In Vitro and in Cultured NIH3T3 Cells

**Robert M. Hernandez, Ginger G. Wescott, Mark W. Mayhew, Meagan A. McJilton, and David M. Terrian***

Department of Anatomy and Cell Biology, Brody School of Medicine, East Carolina University, Greenville, North Carolina 27858

**Abstract** Protein kinase C-epsilon coordinately regulates changes in cell growth and shape. Cells overproducing protein kinase C-epsilon spontaneously acquire a polarized morphology and extend long cellular membrane protrusions that are reminiscent of the morphology observed in *ras*-transformed fibroblasts. Here we report that the regulatory C1 domain contains an actin binding hexapeptide motif that is essential for the morphogenic effects of protein kinase C-epsilon in cultured NIH3T3 murine fibroblasts. The extension of elongate processes by protein kinase C-epsilon transformed fibroblasts appeared to be driven by a kinase-independent mechanism that required organized networks of both actin and microtubules. Flow cytometry of phalloidin-stained cells demonstrated that protein kinase C-epsilon significantly increased the cellular content of polymerized actin in NIH3T3 cells. Studies with a cell-free system suggest that protein kinase C-epsilon inhibits the in vitro disassembly of actin filaments, is capable of desequestering actin monomers from physiologically relevant concentrations of thymosin $\beta_4$, and increases the rate of actin filament elongation by decreasing the critical concentration of actin. Based on these and other observations, it is proposed that protein kinase C-epsilon may function as a terminal downstream effector in at least one of the signaling pathways that mitogens engage to initiate outgrowth of cellular protrusions. J. Cell. Biochem. 83: 532–546, 2001. 

**Key words:** protein kinase C; actin; polymerization; critical concentration; thymosin $\beta_4$; latrunculin B

Protein kinase C epsilon (PKCε) defines a new type of oncogenic, actin binding, protein that is capable of engaging the diverse morphological and functional alterations associated with malignant transformation. PKCε expression promotes the acquisition of a polarized and fusiform morphology, a loss of density-dependent growth regulation, and tumor formation in nude mice [Cacace et al., 1993; Mischak et al., 1993]. The oncogenic potential of PKCε is evident in preneoplastic cells of distinct embryological origin [Cacace et al., 1993; Perletti et al., 1996a,b; Gubina et al., 1998; Lavie et al., 1998; Knauf et al., 1999; Sharif and Sharif, 1999] and certain details pertaining to the molecular basis for this cellular transformation have now begun to emerge. PKCε apparently responds to various enzymes involved in the phosphoinositide cycle [Moriya et al., 1996; Le Good et al., 1998], by activating multiple signal transduction pathways to differentially regulate gene expression [Ohno et al., 1994; Genot et al., 1995; Reifel-Miller et al., 1996; Soh et al., 1999], the production of autocrine growth factors [Cacace et al., 1998], and escape from regulated growth [Mischak et al., 1993]. Recent evidence suggests that growth stimulatory signals downstream of PKCε are most likely to be mediated by mitogen-activated protein kinase activity [Ueffing et al., 1997; Soh et al., 1999]. It is remarkable that, in addition to these potent effects on cellular growth, PKCε can also dramatically alter the cytoskeletal organization and morphology of neuroectodermal cells by inducing an outgrowth of neurite-like extensions [Fagerström et al., 1996]. The fact that these morphogenic effects of PKCε are independent of its catalytic domain [Zeidman et al., 1999] supports the idea that there is a point of divergence in the effector mechanisms downstream of PKCε that function

Grant sponsor: Contract grant sponsor: National Institutes of Health (to DM Terrian); Contract grant number: ES8397.

*Correspondence to: David M. Terrian, Department of Anatomy and Cell Biology, Brody School of Medicine, East Carolina University, Greenville, North Carolina 27858.
E-mail: terriand@mail.ecu.edu

Received 8 May 2001; Accepted 27 June 2001


DOI 10.1002/jcb.1246

in a kinase-dependent and kinase-independent manner to control cell growth and shape, respectively.

We have previously shown that PKCε contains a small actin-binding motif that is unique to this individual member of the PKC gene family and that this hexapeptide is required for the physical interaction between PKCε and filamentous actin, F-actin [Prekeris et al., 1998]. The outgrowth of long cellular extensions by PKCε-transformed fibroblasts was also documented in this earlier report [Prekeris et al., 1998]. Based on the observations that PKCε decreases the critical concentration of actin, while promoting nucleation and filament assembly in a cell-free system, it is now proposed that PKCε may be capable of promoting the generation of a protrusive force(s) required to initiate the outgrowth of long cellular protrusions. Here, we provide evidence that PKCε directly interacts with monomeric G-actin to induce actin polymerization, at low ionic strecngth and in the presence of thymosin $\beta_4$, while also inhibiting F-actin depolymerization. PKCε-transformed fibroblasts form long and narrow processes containing both PKCε and polymerized actin filaments. This significant morphologic alteration persisted in the presence of extensive cell–cell contacts. As in neuroblastoma cells [Zeidman et al., 1999], intact actin and microtubule networks were strictly required for the maintenance of these atypical cellular processes. Moreover, inhibitors of PKC catalytic activity did not alter process extension by PKCε-transformed fibroblasts or the PKCε-induced polymerization of actin in cell-free assays. These studies suggest that a kinase-independent mechanism may account for the remarkable polarization of cell shape that PKCε expression has now been shown to induce in neuronal model systems, such as PC12 [Hundle et al., 1995] and neuroblastoma cells [Zeidman et al., 1999], and in NIH3T3 murine fibroblasts [Prekeris et al., 1998]. More important, a deletion analysis indicates that the actin-binding motif we have previously described [Prekeris et al., 1996, 1998] plays a major role in mediating the morphogenic activity of PKCε in murine fibroblasts.

## METHODS

All reagents used in this study were of the highest grade available and purchased from the Sigma Chemical Co. (St. Louis, MO), unless otherwise indicated. The Sf9 cell line, pFastBac expression vectors, and oligonucleotide primers were purchased from Life Technologies, Inc. (Gaithersburg, MD). Recombinant purified PKCβII, PKCε, and PKCζ were purchased from Panvera (Madison, WI). Synthetic peptides were provided by David G. Klapper (University of North Carolina at Chapel Hill). Antipeptide antisera against the C-terminus of PKCβII, PKCε, and PKCζ were provided by D. Kirk Ways (Lilly Research Laboratories, Indianapolis, IN). Antiactin Antisera was purchased from Amersham Pharmacia Biotech, Inc. (Piscataway, NJ). Rhodamine phalloidin, Texas Red-X phalloidin, and N-(1-pyrene)iodoacetamide were from Molecular Probes (Eugene, OR). Nickel-nitrilotriacetic acid (NiNTA) agarose was obtained from Qiagen (Chatsworth, CA). GF109203X was from Research Biomedicals International (Natick, MA) and 2D-silver stain II was from Daiichi Pure Chemicals Co., LTD (Tokyo, Japan). Latrunculin B was from Alexis Biochemical Corp. (San Diego, CA), Gö 6976 and PD 98059 were from Calbiochem (San Diego, CA), and carbon type-B, 400 mesh, copper grids were from Ted Pella, Inc. (Redding, CA).

### Baculovirus Expression and Purification of PKCε

The subcloning and deletion mutagenesis strategy used to prepare wild-type PKCε, polyhistidine-tagged PKCε ($His_6$-PKCε), and a PKCε mutant containing an internal deletion from codons 1013–1039 of the mouse PKCε gene (corresponding to an actin-binding motif) have been described previously [Prekeris et al., 1998]. The deletion mutant of PKCε has been designated $\Delta PKC\varepsilon^{222-230}$ and was also expressed as a $His_6$-$\Delta PKC\varepsilon^{222-230}$ fusion protein. $His_6$-tagged fusion proteins were purified by metal affinity chromatography using NiNTA-agarose and have previously been shown to be catalytically active and retain specific binding sites for [$^3$H]4β-phorbol 12,13-dibutyrate (PDBu) [Prekeris et al., 1998].

### Generation of Overexpressing Cell Lines

NIH3T3 mouse embryo fibroblasts (ATCC No. CRL 1658) were transduced with an empty pLXSN recombinant retrovirus (3T3-L) or pLXSN harboring genes for PKCε (3T3-Lε) or $\Delta PKC\varepsilon^{222-230}$ (3T3-LΔε), selected using the aminoglycoside antibiotic G418 (500 μg/ml), and

subcloned by limiting dilution as described previously [Prekeris et al., 1998].

### Quantification of Process Morphology Induced by PKCε and $\Delta PKC\varepsilon^{222-230}$

3T3-L, 3T3-Lε, and 3T3-LΔε clonal derivatives ($8.6 \times 10^5$ cells/well) were plated in triplicate onto 100-mm plastic culture dishes in a medium containing 10% bovine calf serum and incubated at 37°C. The frequency of process formation was quantified at the times specified, using unfixed cells, in three to six independent experiments, scoring 200 cells each. Cells bearing processes longer than that of two cell bodies were scored positive. Where indicated, pharmacological and biochemical reagents were added at the specified concentrations, to the culture medium 2 hr after plating the cells. Measurements were converted to micrometers using a micrometer, photographed and viewed at the same magnification.

### Fluorescence Microscopy

Indirect immunofluorescence localization of PKCε was performed as described previously [Prekeris et al., 1998] and the actin cytoskeleton was visualized with rhodamine phalloidin. Cells were visualized with a 100× objective using a Zeiss photomicroscope III.

### Flow Cytometric Assay of Cellular F-actin

Subconfluent cultures of NIH3T3, 3T3-Lε-7, and 3T3-LΔε-9 cells were collected by mild trypsinization and gentle centrifugation, washed twice in PBS, and $1 \times 10^6$ cells were resuspended in a 1 ml solution containing 50 μg lysopalmitoylphosphatidylcholine, 3.7% formaldehyde, and 10 IU of Texas Red-X phalloidin. After a 20-minute incubation at 4°C, the cells were washed three times with PBS and the relative cellular content of F-actin was measured in $1 \times 10^4$ phalloidin-stained cells by flow cytometry (FACScan) at 488 nm excitation, with gating set to exclude debris.

### Actin Preparations

Filamentous α-actin was purified from rabbit skeletal muscle as before [Prekeris et al., 1998]. Monomeric G-actin was generated by dialyzing F-actin for 48 hr against G-buffer (5 mM Tris–HCl, pH 7.6, containing 0.2 mM $CaCl_2$, 0.2 mM ATP, and 0.5 mM β-mercaptoethanol). Residual F-actin was then removed by sedimentation at 100,000*g* for 1 hr. G-actin was labeled with N-(1-pyrene) iodoacetamide as described by Kouyama and Mihashi [1981]. Briefly, F-actin was diluted to 1 mg/ml with 2 mM Tris–HCl, pH 7.6, containing 100 mM KCl, 1 mM $MgCl_2$, 0.2 mM $CaCl_2$, and 0.2 mM ATP. N-(1-pyrene)iodoacetamide was then added to a final concentration of 23.3 μM and reactants were wrapped in aluminum foil and incubated for 20 hr at 4°C. After a 48-hour dialysis against G-buffer, the soluble pyrene-labeled G-actin was obtained from 100,000*g* (1 hr) supernatants.

### Actin Polymerization by Fluorescence Spectroscopy

G-actin (5 μM, 1:10 pyrene-labeled) was converted to $Mg^{2+}$-actin by the addition of 125 μM EGTA and 50 μM $MgCl_2$, and after 15 min was incubated for an additional 5 min at 23°C in the absence or presence of the specified concentrations for recombinant $His_6$-PKCε or a synthetic thymosin $\beta_4$, lacking only the N-terminus Met residue. Raising the concentrations of KCl and $MgCl_2$ to 60 mM and 1 mM, respectively, induced polymerization. Changes in fluorescence intensity were measured at Ex 345 nm and Em 385 nm using an LS-50B Perkin–Elmer luminescence spectrometer. The critical concentration for actin polymerization was estimated by measuring the fluorescence of varying concentrations of pyrene-labeled actin (1–9 μM), 4 hr after the addition of 0.35 mM $MgCl_2$, in the absence and presence of $His_6$-PKCε (0.1 or 0.3 μM). The $MgCl_2$ concentration of 0.35 mM was chosen to provide an artificially high critical concentration in the absence of PKCε, so that any decreases caused by this recombinant protein could be accurately measured. In depolymerization assays, 1 μM G-actin (1:10 pyrene-labeled) was allowed to polymerize 3 hr before adding PDBu (500 nM) and increasing concentrations of recombinant $His_6$-PKCε or BSA. The PDBu was added to this mixture in order to expose the actin-binding motif of PKCε, which appears to be partially cryptic when this kinase is in an inactive conformation [Prekeris et al., 1996, 1998]. After 15 min, all samples were diluted 12-fold (final 5 mM KCl) and the rate of actin depolymerization was monitored for 30 min. Increases in ionic strength resulting from the addition of $His_6$-PKCε were monitored using a conductivity meter (Bio-Rad Laboratories, Hercules, CA); 1 μM $His_6$-PKCε was equivalent to a final concentration of 15 mM KCl (data not shown).

### Electrophoretic Mobility Shift Assays (EMSA)

A 300-nM final concentration of G-actin was preincubated for 10 min at 37°C in G-buffer and in the absence or presence of the synthetic hexapeptide LKKQET (10 μM) or GF109203X (1 μM). Recombinant $His_6$-PKCε (200 nM) or BSA (1 μM) was then added in the presence of 500 nM PDBu or an equimolar concentration of the inactive PDBu isomer, 4α-PDBu. Samples were equilibrated 30 min at 37°C and analyzed by PAGE under nondenaturing conditions (N-PAGE), according to the method of Safer (1989), and visualized using Daiichi Silver Stain II.

### Coimmunoprecipitation

Purified recombinant $His_6$-PKCε (1 μM) was coincubated with PDBu (500 nM) and G-actin (5 μM) in a G-buffer for 15 min at 23°C. Equal aliquots of this mixture were transferred to separate tubes and anti-PKCε monoclonal antisera (Transduction Laboratories, Lexington, KY) was added to one of these samples at a final concentration of 1:50 (v/v). After 4 hr of incubation on a rocker at 4°C, the secondary anti-mouse IgG and protein A-agarose were added to each sample and incubation at 4°C was continued for 1 hr. Agarose beads and immunoprecipitates were sedimented (5,000*g*, 5 min) and washed three times with excess G-buffer. Each immunoprecipitate and supernatant fraction was collected and solubilized in hot (45°C) sample buffer [Prekeris et al., 1996] for Western blot analysis using anti-PKCε and Antiactin Antisera.

### Actin Cosedimentation

While assessing the binding of $His_6$-PKCε to G-actin, we observed a consistent rise in sample viscosity and this was confirmed using a standard falling ball viscometry assay (data not shown). To determine whether this increased viscosity might be due to PKCε induced polymerization of G-actin, actin cosedimentation assays were performed using monomeric G-actin in a G-buffer. Protocols and additions tested in each experiment were as specified below. Typically, this involved the coincubation of G-actin (5 μM) and the recombinant PKC isoform (1 μM) indicated for 4 hr at 23°C in the presence of 500 nM PDBu. Soluble (G-actin) and insoluble (F-actin) actin were then separated by centrifugation (100,000*g*, 1 hr) and analyzed by SDS-PAGE and protein staining with Coomassie Brilliant Blue or Daiichi Silver Stain II.

### Electron Microscopy

G-actin (5 μM) was coincubated 4 hr at 23°C in a G-buffer containing PDBu (500 nM) in the absence or presence of $His_6$-PKCε (1 μM). Aliquots of this protein mixture were diluted 1:1 (v/v) with G-buffer and applied to carbon type-B grids. Adsorbed proteins were then stained with 1% uranyl acetate for 30 s and visually inspected using a JEOL 1200 electron microscope.

### Data Analysis

All results shown are representative of duplicate or triplicate determinations from at least three independent experiments. Treatment effects were only evaluated for statistical significance ($P < 0.05$; two-sided Student's $t$ test) using the data shown in Figures 2A, 4A, and 5, and Table I. Adobe Photoshop 5.0 software was used to prepare all digital images and micrographs presented in this report.

## RESULTS

### Characterization of NIH3T3 Murine Fibroblasts That Overproduce PKCε or a Deletion Mutant Lacking an Actin-Binding Site Within the C1 Domain

We have performed a series of reversion assays using 3T3-Lε and 3T3-LΔε cell lines in an attempt to discern how PKCε might interact with actin to regulate the behavior of cells. A detailed explanation of the methods used to establish these clonal derivatives, and the corresponding vector controls, has been provided [Prekeris et al., 1998]. As the assays reported here were based on morphological phenotype, it was essential that all cell lines examined retain transfected plasmid sequences during a limited number of passages in culture. For this reason, all clonal derivatives were maintained in G418 (100 μg/ml) as early passage cells and Western blot analyses routinely used to confirm the retention and expression of the pLXSN–PKCε constructs. As shown in Figure 1A, expression levels remained significantly elevated in several of the 3T3-Lε and 3T3-LΔε cell lines after 5–6 passages in culture. In other studies, we have confirmed that 3T3-Lε and 3T3-LΔε cell lines both grow efficiently in

**TABLE I. Summary of the Effects of Pharmacological and Biochemical Reagents on the Induction/Maintenance of Long Filopodial Extensions**

| | Frequency of process formation by 3T3-Lε-7 cells (percent of untreated controls) | | | |
|---|---|---|---|---|
| | Duration of exposure (hr) | | | |
| Reagent tested | 1 | 2 | 3 | 4 |
| Inhibitors of actin polymerization | | | | |
| Latrunculin B (200 nM) | 98 | 43 | 29 | 27 |
| Cytochalasin B (1 μM) | 16 | 14 | 7 | 0 |
| Microtubule destabilizing agents | | | | |
| Nocodazole (1 μM) | 75 | 19 | 15 | 2 |
| Vincristine (1 μM) | 42 | 18 | 4 | 0 |
| Reagents that alter protein phosphorylation | | | | |
| GF-109203X (500 nM) | 108 | 92 | 94 | 89 |
| Gö 6976 (100 nM) | 126 | 94 | 96 | 91 |
| PD 98059 (50 μM) | 96 | 86 | 87 | 84 |
| Genistein (25 μM) | 83 | 81 | 84 | 82 |
| Okadaic acid (100 nM) | 91 | 52 | 51 | 51 |
| Wortmannin (100 nM) | 64 | 68 | 60 | 55 |
| Serum-withdrawl | 98 | 94 | 64 | 64 |

3T3-Lε-7 cells ($8.6 \times 10^5$ cells) were plated in triplicate onto 100-mm plastic culture dishes in medium containing 10% boviné calf serum and incubated for 2 hr at 37°C. Reagents were then added to two of the culture dishes, at the specified concentration, or the concentration of bovine serum was reduced to 0.5%. The third culture dish served as an untreated control for each of the reagents tested. The frequency of process formation in the absence and presence of each reagent was quantified at the times specified, scoring 200 cells per dish every hour. Cells bearing processes longer than that of two cell bodies were scored positive. The effects of these reagents were simultaneously tested on 3T3-L and 3T3-LΔε-9 cells under identical conditions. With the exception of latrunculin B (Fig. 3),the morphological effects of these reagents were similar in the three cell lines tested. Data are expressed as a percentage of the paired untreated control and are means from three independent experiments.

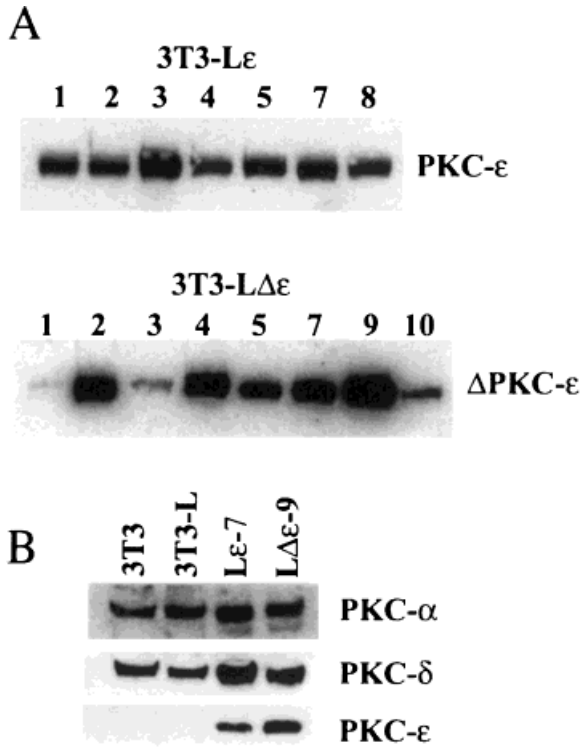


**Fig. 1.** Western blot analysis of PKC expression in PKCε and ΔPKCε $^{222-230}$ overproducing cell lines. **A:** Equivalent amounts of total protein from the indicated 3T3-Lε (wt PKCε) or 3T3-LΔε (ΔPKCε) clonal derivatives (1–10) were analyzed by SDS-PAGE and immunoblotted with antipeptide antisera against the C-terminus of PKCε. **B:** Equivalent amounts of protein (30 μg) from parental NIH3T3 cells (3T3), pLXSN vector controls (3T3-L), and the specified PKCε (Lε) and ΔPKCε $^{222-230}$ (LΔε9) clones were analyzed by SDS-PAGE and immunoblotted with the specified antipeptide antisera against the C-terminus of PKCα, PKC, or PKCε.

soft agar and are tumorigenic in nude mice (data not shown). Thus, a spontaneous reversion of transformation is unlikely to account for the revertant 3T3-LΔε clones presented below in this report. Furthermore, the parental NIH3T3 cells and vector control lines used in the present study only expressed detectable amounts of PKCα and PKCδ; PKCζ was not detected and the endogenous expressions of PKCα and PKCδ were not substantially altered by the ectopic expression of either PKCε or ΔPKCε$^{222-230}$ (Fig. 1B). These results indicate that heterologous changes in the endogenous expression of PKC isoforms were not required to establish or maintain the phenotypic characteristics of 3T3-Lε and 3T3-LΔε cells.

### Occlusion of the PKCε-transformed Morphotype in NIH3T3 Cells

The control cell line 3T3-L displayed a morphology that was characteristic of the parental NIH3T3 cells at subconfluence. In contrast, clonal derivatives that expressed high levels of PKCε, 3T3-Lε clones 5, 7, and 8 (Fig. 1A), spontaneously began to form long and narrow cellular processes within 3 hr of replating onto tissue culture plastic (Fig. 2A). The acquisition of this morphotype was consistently observed in the presence of 10% bovine serum and did not require the addition of supplementary PKC agonists. After 6 hr, the frequency of process formation had increased to $44 \pm 5\%$ of all cells (Fig. 2A). By this time, processes had extended over a distance

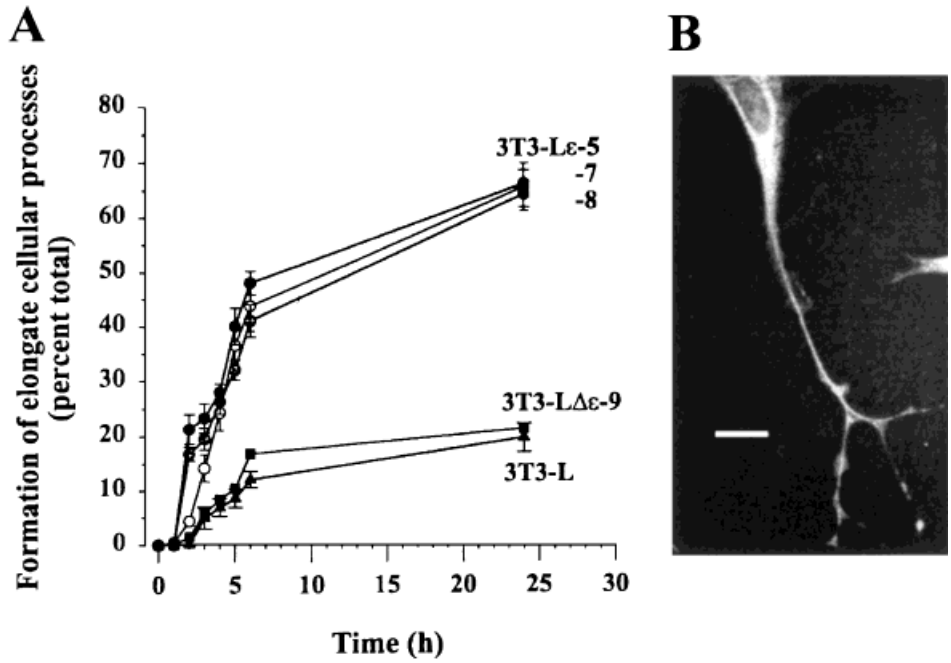


**Fig. 2.** Process formation by PKCε overproducing cell lines. **A:** Time course of process formation. Increases in the number of process bearing cells were quantified using subconfluent (40–60% at plating) cultures of the cell lines specified. PKCε overproducing cell lines begin to establish elongate processes, at least two cell bodies in length, within 2 hr of plating; their frequency of appearance continued to increase for 24 hr. Cells overexpressing ΔPKCε $^{222-230}$ (3T3-LΔε-9) behaved similar to the vector controls (3T3-L), with fewer than 20% of all cells counted (200 cells) bearing elongate processes after 24 hr in culture. Data are the mean±SEM of triplicate determinations in three to six independent experiments. **B:** Immunofluorescence microscopy of a typical 3T3-Lε-7 cell stained with anti-PKCε antibodies 6 hr after replating onto tissue culture plastic. 3T3-Lε-7 fibroblasts established elongate and branching cellular protrusions with multiple en passant swellings that were immunopositive for PKCε. Bar, 5 μm.

of 40–80 μm, with numerous en passant swellings and branches that were immunopositive for PKC-ε staining (Fig. 2B). The colocalization of PKC-ε and F-actin within these cell processes has previously been demonstrated [Prekeris et al., 1998]. The frequency and length of cellular processes continued to grow at high cell densities, such that 65±4% of the 3T3-Lε cells had formed elongate processes within 24 hr (Fig. 2A). At 48 hr after plating, PKCε-transformed 3T3-Lε fibroblasts began forming foci and continued to exhibit elongated processes. It was evident from the extensive network of overlapping processes and cell bodies that the extension of these processes was not contact inhibited in these confluent cultures. Deletion of the actin-binding motif within the C1 domain of PKCε resulted in a profound occlusion of the PKCε-transformed morphotype (Fig. 2A). As a high level of PKCε expression is required to observe morphogenic effects in subconfluent rodent fibroblasts [Cacace et al., 1993], it is important to note that the levels of transcript expression were roughly equivalent in the 3T3-Lε-7 cells and 3T3-LΔε-9 clones used in these experiments (Fig. 1B).

### Process Extension Requires Organized Actin and Microtubule Networks

The actin-disrupting agent latrunculin B was used to determine if PKCε regulates the actin filament dynamics required for active extension of elongate cellular processes in intact cells. Each cell line was replated at a cell density of 40–60% and grown for 24 hr in the absence of toxin, thus allowing cells to elaborate networks of extended processes (Fig. 2A). Within 20 min of treatment with 800 nM latrunculin B, the vector control 3T3-L and 3T3-LΔε-9 cell lines had all become highly rounded (Table I). In contrast, while cell shrinkage was evident, the 3T3-Lε-7 fibroblasts continued to exhibit cellular extensions and immunofluorescence microscopy indicated that these processes contained both PKC-ε and filamentous actin. This evidence suggests that PKCε may be capable of productively interacting with actin in the presence of latrunculin B, a potent actin monomer

sequestering molecule. However, even the 3T3-Lε-7 clones ceased to elaborate new processes and began rounding up after a more prolonged exposure (3 hr) to latrunculin B (Table I). Interestingly, PKCε overproduction provided no protection from an alternative toxin that also interferes with actin polymerization, cytochalasin B. This agent interacts with the barbed end of actin filaments at low concentrations and will also bind to actin monomers at higher doses [Cooper, 1987]. Within 1 hr, 1 μM cytochalasin B had caused all cell lines to become completely rounded and the frequency of process formation decreased by at least 80% (Table I data not shown). The effects of these two reagents, and their distinct modes of action, imply that PKCε may interact with preexisting filaments to decrease the off-rate at pointed ends and, thereby, forestall the capture of actin monomers by these sequestering agents. The efficacy of cytochalasin B suggests that uncapped growth sites may also be required for process formation in PKCε-transformed fibroblasts.

Cellular processes elaborated by *ras*-transformed fibroblasts gradually retract in the presence of nocodazole [Shelden, 1999], an inhibitor of microtubule assembly. 3T3-Lε-7 cells displayed a similar morphogenic response to the microtubule inhibitors nocodazole and vincristine (Table I). Within 2 hr of treatment, the typically long and narrow processes collapsed into much shorter ($< 20$ μm) and thickened ($\sim 10$ μm) extensions that persisted in the continued presence of these drugs for up to 6 hr. These observations support the idea that transformed NIH3T3 cells must be able to assemble newly polymerized networks of both actin and microtubules in order to establish and maintain process extensions in culture.

Several additional reagents have now been tested for morphogenic effects on the initiation, elongation, and maintenance of cellular processes by 3T3-Lε overexpressing clonal derivatives. Most notably, we have found that bisindoylmaleimide derivatives that inhibit either all PKCs (GF-109203 X; 500 nM), or preferentially inhibit conventional isoforms (Gö 6976; 100 nM), did not alter the frequency of process formation or the morphology of such processes. These agents were tested solely to confirm the convincing demonstration that the morphogenic effects of PKCε are resident within the N-terminal regulatory domain and entirely independent of its catalytic C-terminus [Zeidman et al., 1999]. Other treatments that did not significantly affect process formation in 3T3-Lε-7 cells included the MEK kinase inhibitor PD 98059 (50 μM) and the tyrosine kinase inhibitor genistein (25 μM). Finally, a protein phosphatase inhibitor, okadaic acid, an inhibitor of PI 3-kinase, wortmannin, and serum withdrawal significantly reduced the frequency of process formation by 3T3-Lε-7 cells within 3 hr of treatment. Together, these data suggest that a protein phosphatase type 1 and/or 2A, 3-phosphoinositides, and growth factors may participate in the regulation of actin dynamics by PKCε.

### PKCε Increases the Content of Phalloidin-Stained Actin in Individual Cells

Flow cytometry was used to gain a more quantitative estimate of the effects that constitutively expressing PKCε, or its deletion mutant might have on the relative content of F-actin within individual NIH3T3 fibroblasts. NIH3T3, 3T3-Lε-7, and 3T3-LΔε-9 sublines were prepared for flow cytometric analysis of F-actin by simultaneous fixation, permeabilization, and fluorescent phallotoxin staining, according to the manufacturer's protocol (see Methods). This analysis revealed that the mean relative fluorescence intensity (MRFI) of phalloidin-stained 3T3-Lε-7 cells ($1 \times 10^4$) was increased by 70% over that of the parental NIH3T3 fibroblasts and, importantly, the MRFI of 3T3-LΔε-9 cells was equivalent to the NIH3T3 controls (Fig. 3A). This increase in the MRFI of 3T3-Lε-7 cells could not be accounted for by an increase in cell size as the forward scattering properties of 3T3-Lε-7 and 3T3-LΔε-9 cells did not differ on the flow cytometer (data not shown). Thus, this result provided an important independent line of evidence that the intracellular concentration of PKCε was sufficient to increase the cellular content of polymerized actin in cultured 3T3-Lε fibroblasts. Moreover, the data indicated that a small cluster of charged amino acids (LKKQET) within the C1 domain of PKCε played a crucial role in mediating the interaction between PKCε and the actin-based cytoskeleton.

### PKCε Inhibits the In Vitro Disassembly of Actin Filaments

The accumulating evidence that PKCε was an actin-binding protein with kinase-independent effects on cell morphology raised the question of

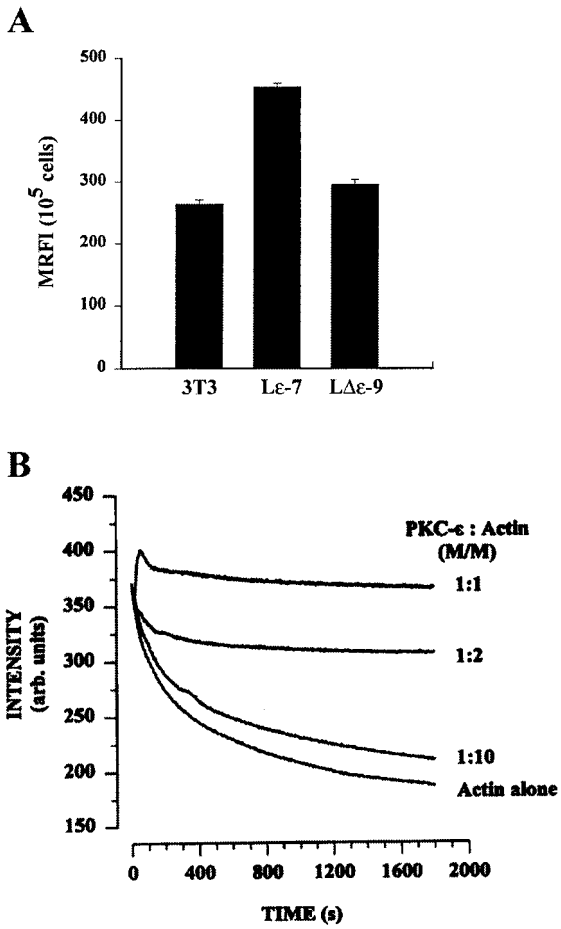


**Fig. 3.** In vivo and in vitro effects of PKCε on actin assembly. **A:** Overexpression of PKCε, but not ΔPKCε $^{222-230}$, increased the mean relative fluorescence intensity (MRFI) of phallotoxin-stained NIH3T3 cells. Subconfluent NIH3T3, 3T3-Lε-7, and 3T3-LΔε-9 cell cultures were brought into suspension by mild trypsinization and simultaneously fixed, permeabilized, and stained using a mixture of formaldehyde, lysopalmitoylphosphatidylcholine, and fluorescent phallotoxin, respectively. The relative cellular content of F-actin was measured by recording the MRFI of $1 \times 10^4$ phalloidin-stained cells on a flow cytometer. Data are the mean±SEM of triplicate determinations. **B:** Increasing amounts of recombinant PKCε prevented the in vitro disassembly of actin filaments. Pyrenyl-G-actin (1 μM; 10% labeled) was allowed to polymerize in the dark for 3 hr in the presence of 60 mM KCl and 1 mM $MgCl_2$ before adding PDBu (500 nM) and increasing amounts of PKCε. The final molar ratio of total PKCε to total actin is as specified. After 15 min at ambient temperature, all samples were diluted with G-buffer to a final concentration of 5 mM KCl; the resultant actin depolymerization was monitored by fluorescence spectroscopy. The structure of actin polymers was normal in samples diluted in the presence of equimolar concentrations of PKCε and actin (electron microscopic images not shown). All curves are representative of three independent experiments.

whether PKCε directly interacted with actin to regulate cytoskeletal function. As a first approach to gaining insight into this issue, we examined the in vitro effects of recombinant PKCε on the stability of purified actin polymers. Pyrenyl-F-actin was used as an optical probe to monitor changes in the amount of F-actin. Actin filaments polymerized in F-buffer (G-buffer + 60 mM KCl and 1 mM $MgCl_2$) rapidly disassembled after diluting the KCl concentration to 5 mM with G-buffer (Fig. 3B). Adding recombinant PKCε before dilution effectively inhibited the depolymerization of actin polymers under these conditions (Fig. 3B). Conductivity measurements confirmed that the addition of 1 μM PKCε did not increase the overall ionic strength of the diluted assay buffer (data not shown). These data reveal that PKCε is capable of stabilizing actin oligomers under these in vitro conditions.

### PKCε Increases the Rate of Actin Filament Elongation and Decreases the Critical Concentration of Actin

Figure 4A shows the polymerization of 5 μM G-actin (10% pyrene-labeled), in the absence and presence of PKCε, following the addition of F-buffer to the reaction mixture. This analysis revealed that PKCε significantly increased the rate of actin polymer elongation when the molar ratio of total PKCε to total actin was 0.2. A decrease in the initial lag phase of polymerization was consistently observed (Fig. 4A; insert), providing the first indication that PKCε may interact with actin monomers to promote the growth/elongation of new filaments. In contrast, 1 μM ΔPKCε $^{222-230}$ did not alter the rate of actin polymerization under these conditions (not shown). The data shown in Figure 4B indicate that PKCε may influence the rate of polymerization by lowering the critical concentration of actin. In the presence of a low concentration of $MgCl_2$ (0.35 mM), the critical concentration of actin was estimated to be 4.2 μM and this value was reduced to 2.4 and 0.2 μM within 4 hr after the addition of 0.1 and 0.3 μM PKCε, respectively (Fig. 4B).

### PKCε Surmounts the Inhibition of Actin Nucleation by Thymosin $\beta_4$

The possibility that PKCε might be capable of desequestering ATP-G-actin from a thymosin $\beta_4$ –G-actin complex prompted us to examine PKCε-actin interactions in the presence of a

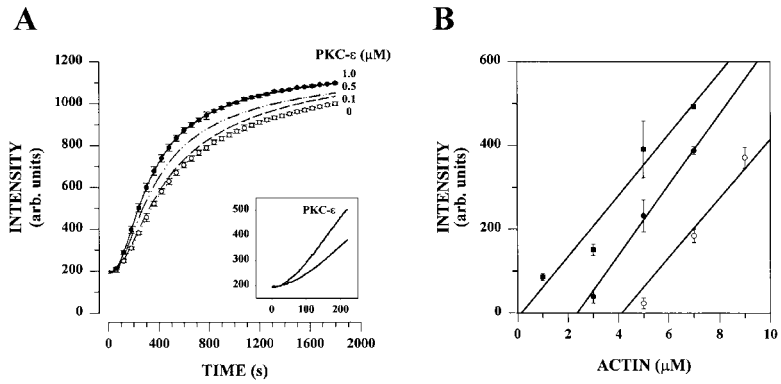


**Fig. 4.** Recombinant PKCε increased the rate of actin polymerization and lowered the critical concentration of actin. **A:** Time course of pyrenyl-actin polymerization in the absence and presence of purified recombinant PKCε and 500 nM PDBu. The specified final concentration of PKCε was added to 5 μM pyrenyl-actin (10% labeled) in G-buffer immediately prior to inducing actin polymerization with a further addition of KCl and $MgCl_2$ to final concentrations of 60 mM and 1 mM, respectively. Fluorescence intensity was monitored at Ex 345 nm and Em 385 nm. Bars are standard deviations for three independent experiments. **Inset.** Initial rate of actin polymerization in the presence of 0 and 1 μM PKCε. **B**: Critical concentration of actin at steady-state equilibrium in the absence and presence of PKCε. Varying concentrations of $Mg^{2+}$-actin (5% pyrene-labeled) were incubated 4 hr in the presence of 0.35 mM $MgCl_2$ and 0 (○), 0.1 μM (●), or 0.3 μM (■) PKCε. Data are the mean±SEM of triplicate determinations in three independent experiments.

biologically relevant concentration of synthetic thymosin $\beta_4$ (300 μM). As shown in Figure 5, synthetic thymosin $\beta_4$ exhibited the native ability of this tetradecadipeptide to sequester ATP-G-actin and inhibit actin nucleation. Moreover, PKCε proved to be remarkably effective in reclaiming G-actin from this concentrated pool of thymosin $\beta_4$. Indeed, actin polymerization was restored to a significant extent when the molar ratio of total PKCε to total thymosin $\beta_4$ was exceptionally low (0.003; Fig. 5).

### PKCε Interacts With Actin Monomers to Promote Actin Polymerization

It has been shown that PKCε binds F-actin [Prekeris et al., 1998], but this would not explain how PKCε was able to reclaim actin monomers from the thymosin $\beta_4$–G-actin pool. Therefore, we have examined the interactions between PKCε and monomeric actin at an ionic strength that would normally cause depolymerization (e.g., in a G-buffer, see Fig. 3B). Figure 6 illustrates three independent lines of evidence that support a model whereby PKCε interacts with actin monomers to promote the nucleation and elongation of new filaments. First, electrophoretic mobility shift assays (EMSA) indicated that PKCε could promote filament elongation from actin monomers (Fig. 6A, lanes 2 and 3). Multiple bands of decreasing electrophoretic mobility were repeatedly observed each time G-actin (0.3 μM) was coincubated with PKCε (0.2 μM) in a G-buffer (30 min at 37°C). This effect of PKCε (lane 1 vs. lane 2) was enhanced by the addition of 500 nM PDBu (lane 2 vs. lane 3), and was only partially inhibited by a synthetic peptide that is identical to murine PKCε amino acid residues 222–227, LKKQET (10 μM, lane 4), or the PKC inhibitor GF109203X (1 μM, lane 6). The synthetic hexapeptide LKKQET was not sufficient to induce the multimerization of actin monomers

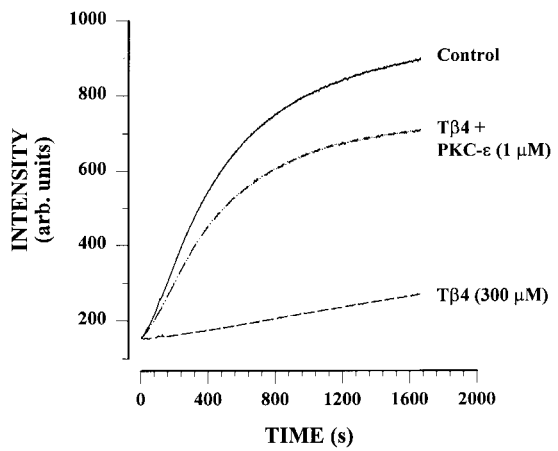


**Fig. 5.** PKCε promoted actin polymerization in the presence of synthetic thymosin $\beta_4$. PKCε desequestered actin from the thymosin $\beta_4$-G–actin complex at a molar ratio of total PKCε to total synthetic thymosin $\beta_4$ of 0.003. The salt-induced polymerization of pyrenyl-actin was initiated and monitored as in Figure 4A in the absence (Control) or presence of 300 μM thymosin $\beta_4$ and 1 μM PKCε, as specified. All curves are representative of three independent experiments.

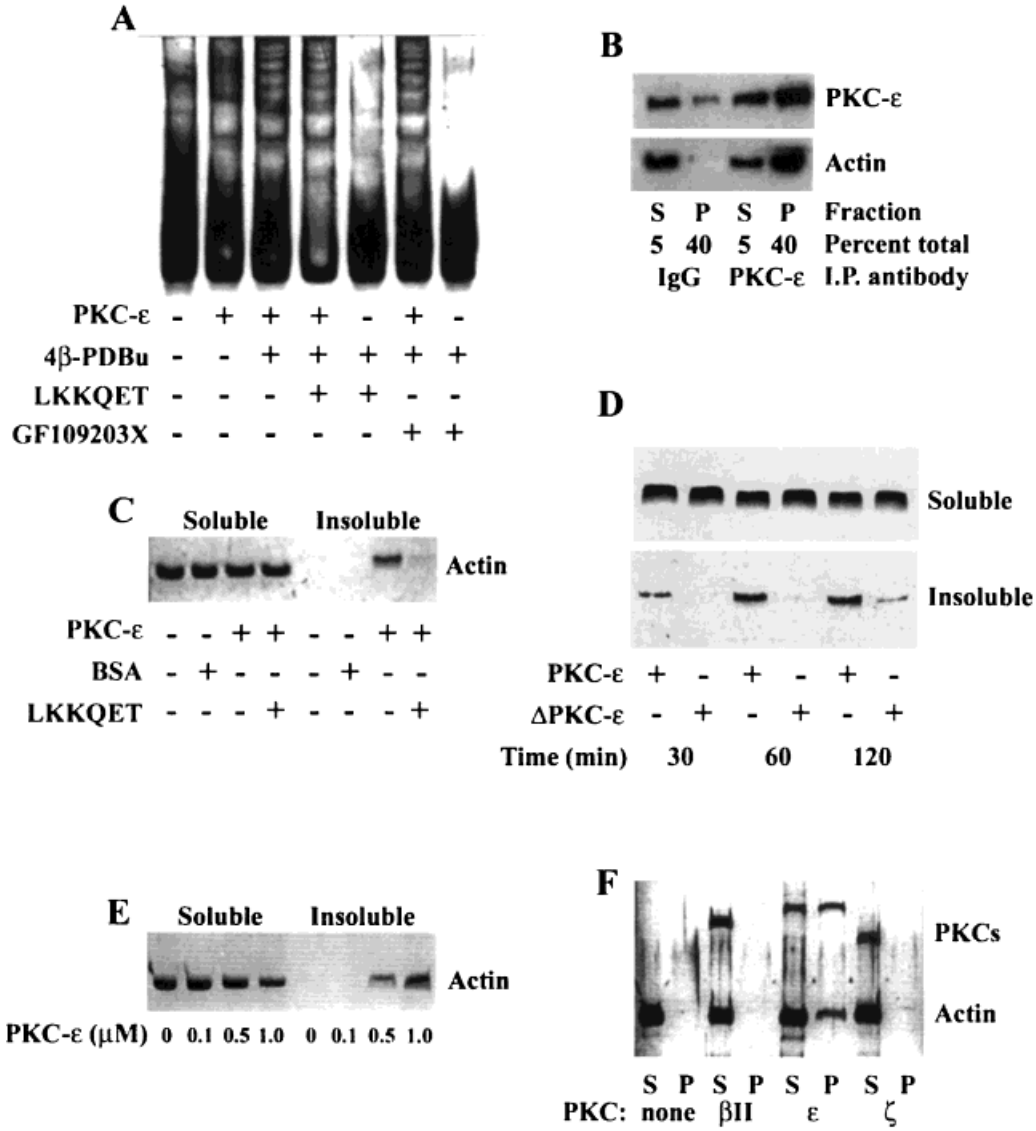


**Fig. 6.** PKCε promoted actin polymer elongation in a G-buffer of low ionic strength. **A**: EMSA assays performed under nondenaturing conditions revealed the formation of multimeric protein complexes when recombinant PKCε (0.2 μM) was coincubated with purified ATP-G-actin (0.3 μM) in a G-buffer for 30 min at 37°C. These protein–protein interactions were more evident in the presence of PDBu (500 nM) and were not prevented by addition of the synthetic hexapeptide LKKQET (10 μM) or PKC inhibitor GF109203X (1 μM). Protein bands were detected using Daiichi Silver stain II. **B**: Immunoprecipitation assays consistently showed coprecipitation of purified G-actin (0.5 μM) and PKCε (0.2 μM) with antipeptide antibodies raised against the C-terminal V5 domain of PKCε (lane 4). Control samples were incubated with the secondary IgG alone (lanes 1 and 2). The soluble protein mixture (S; 5% total) and immunoprecipitates (P; 40% total) were analyzed by SDS-PAGE and immunoblotting with PKCε or actin-specific antibodies. **C**: Sedimentation assays indicated that recombinant PKCε (1 μM) decreased the solubility of G-actin (5 μM) in a G-buffer in the absence, but not the presence, of the synthetic hexapeptide LKKQET (20 μM). PDBu (500 nM) was present in all samples and BSA (18 μM, lanes 2 and 6) was used as a negative control. Soluble and insoluble actin was separated by centrifugation (100,000*g* for 20 min) and analyzed by SDS-PAGE and protein staining with Coomassie Brilliant Blue. **D**: Recombinant ΔPKCε $^{222-230}$ was relatively ineffective in lowering the solubility of actin in a G-buffer. Equimolar concentrations of PKCε and ΔPKCε $^{222-230}$ (1 μM) were incubated with 5 μM G-actin for 30, 60, or 120 min at 23°C in the presence of 500 nM PDBu. Soluble (top panel) and insoluble (bottom panel) actin was detected by protein staining with Coomassie Brilliant Blue. **E:** The solubility of actin (5 μM) in a G-buffer was progressively decreased by increasing concentrations of PKCε (0-1 μM). All samples were incubated 2 hr at 23°C and contained 500 nM PDBu. Soluble and insoluble actin was separated by centrifugation (100,000*g* for 20 min) and analyzed by SDS-PAGE and protein staining with Coomassie Brilliant Blue. **F:** Recombinant $PKC\beta_{II}$ and PKCζ did not alter the solubility of actin in a buffer of low ionic strength. Equimolar concentrations of $PKC\beta_{II}$, PKCε, and PKCζ (1 μM; Panvera, Madison, WI) were incubated with 5 μM G-actin for 2 hr at 23°C in the presence of 500 nM PDBu. Soluble and insoluble PKC and actin were analyzed by SDS-PAGE and protein staining with Daiichi Silver stain II.

under these conditions (lane 5), implying that the actin-binding site we have identified is essential but may not be sufficient to induce actin polymerization (also see Fig. 6D). In a G-buffer, PKCε remained soluble in the absence of actin and polymer gelation was not observed in these assays. Second, coimmunoprecipitation assays demonstrated that in a G-buffer monomeric actin (0.5 μM) formed a stable complex with PKCε (0.2 μM) that could be immunoprecipitated with antibodies raised against the C-terminus of PKCε (Fig. 6B). G-actin did not coprecipitate with PKCε in control samples that were incubated with the secondary IgG alone. Third, a series of actin sedimentation assays were performed to determine whether PKCε could decrease the solubility of G-actin to the extent that actin polymers could be sedimented at a speed of 100,000*g*. In Figure 6C it is shown that 1 μM PKCε, but not BSA (18 μM), decreased the solubility of 5 μM G-actin to this extent. This PKCε induced decrease in actin solubility was blocked by the synthetic peptide LKKQET (20 μM; Fig. 6C, lane 8) to the reaction mixture and was not diminished by synthetic thymosin $\beta_4$ (300 μM, gel not shown). In the presence of 500 nM PDBu, equimolar concentrations of PKCε and $\Delta$PKCε$^{222-230}$ (1 μM) both reduced the solubility of actin under these conditions (Fig. 6D). However, there were clear distinctions between the in vitro activities of the wild-type and mutant proteins in this assay. In the presence of PKCε, actin polymers could be detected within 30 min and the extent of actin polymerization was more substantial at all times examined (Fig. 6D). By varying the concentration of PKCε added to a fixed concentration of G-actin (5 μM) during a 2-hour coincubation, it was determined that a molar ratio of PKCε to actin as low as 1:10 was sufficient to induce actin polymerization in a G-buffer containing 500 nM PDBu (Fig. 6E). When equimolar concentrations of commercially prepared recombinant PKCβII, PKCε, and PKCζ (1 μM) were coincubated with G-actin (5 μM) under identical conditions, it was observed that PKCε was the only putative actin-binding isoform of PKC to form an insoluble complex with purified actin (Fig. 6F, lane 6). However, we note that the PKCε obtained from this commercial source was not as active in this assay as the protein fractions prepared locally, possibly due to differences in the storage buffers used (50 vs. 20% glycerol in the Panvera and local storage buffers, respectively). Finally, low speed sedimentation analysis [Rybakova et al., 1996] indicated that recombinant PKCε, protein did not cross-link actin filaments into supermolecular networks or bundles (Fig. 7 data not shown).

Fluorimetric assays of pyrenyl-actin polymerization independently confirmed that G-actin (5 μM) had polymerized to F-actin in a buffer of low ionic strength and in the presence of recombinant PKCε (1 μM). Under these conditions, the polymerization of actin did not plateau until $\approx$60 min following the addition of PKCε to the reaction medium. To directly examine the physical nature of actin polymers grown in the presence of PKCε, 5 μM G-actin was polymerized to F-actin in a G-buffer containing 1 μM PKCε and then negatively stained with uranyl acetate for examination with an electron microscope (Fig. 7). The actin filaments that were apparent in these preparations had a diameter of 10 nm and the "hollow" appearance that is characteristic of α-helical fibers. No F-actin bundles or cross-linked aggregates were observed when actin was polymerized in the presence of PKCε (Fig. 7) and no actin filaments were formed in the absence of PKCε and therefore are not shown. Finally, recombinant PKCε remained soluble in G-buffer and no fibrillar aggregates could be detected in the absence of purified actin, although decreases in PKCε solubility have been observed in low pH $< 6.0$) environments.

## DISCUSSION

A fascinating reciprocity in the binary interactions between PKCε and actin has now become evident. Studies with a cell-free system have led to the recent discovery that the C-terminus of F-actin is capable of directly stimulating PKCε phosphotransferase activity [Prekeris et al., 1998], while the present evidence introduces the possibility that PKCε promotes the stabilization and elongation of actin filaments by a kinase-independent mechanism. Elemental features of the molecular interactions that may govern these protein–protein interactions have yet to be proposed. However, the principal interface between PKCε and actin has now been mapped to a small cluster of highly charged amino acids in the regulatory C1 domain of PKCε [Prekeris et al., 1996, 1998]. Moreover, a fundamental step

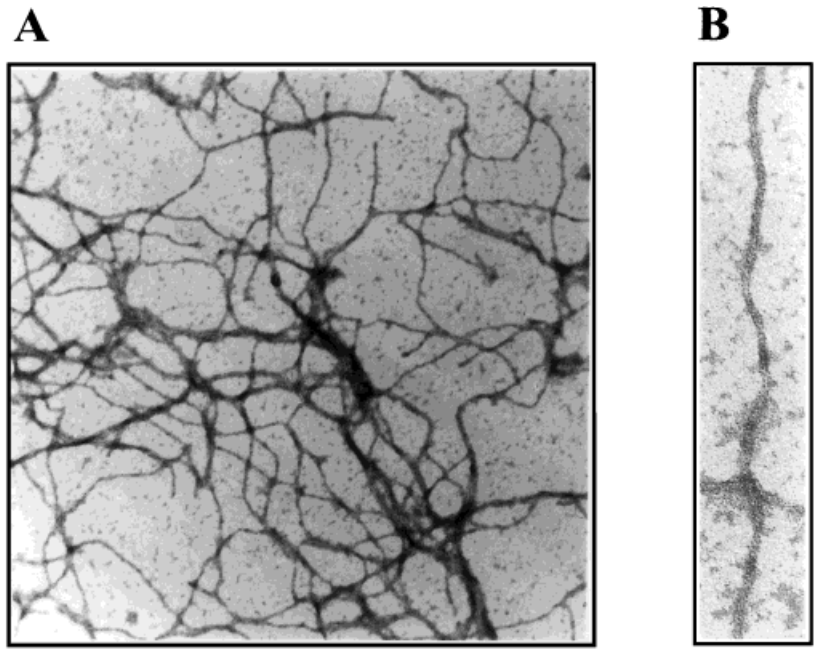


**Fig. 7.** Visual inspection of PKCε-actin polymers. Electron microscopic analysis of actin filaments assembled in a G-buffer containing only recombinant PKCε (1 μM) and purified actin (5 μM). This binary reaction was carried out for 4 hr at 23°C before removing aliquots of the mixture for ultrastructural inspection. Actin polymerized into filaments of the characteristic diameter (8–11 nm) without bundling under these conditions. Magnifications are 75,000× (**A**) and 175,000× (**B**), respectively.

toward understanding how PKCε might regulate cell shape by productively interacting with actin in living cells has now been taken, with the recognition that this actin binding site and actin polymerization are both essential for the morphogenic effects of PKCε in cultured NIH3T3 fibroblasts.

PKCε-transformed murine fibroblasts rapidly acquire a bipolar morphology, and extensive elongations of the cell membrane, after attaching to plastic culture dishes. The idea that there may be a causal relationship between PKCε expression, actin polymerization, and membrane protrusion now seems tenable for several reasons. In individual living cells, the constitutive expression of PKCε significantly increased the content of phallotoxin-stained actin (F-actin) and our in vitro assays provide convincing and direct evidence that PKCε was capable of lowering the critical concentration of actin and the de novo polymerization of actin filaments at a molar ratio of 1:10 (PKCε:G-actin). The concentration of PKCε in 3T3-Lε-7 cells is estimated to be 1 μM (semiquantitative Western blot analyses performed with cell lysates and recombinant PKCε, data not shown) and may, therefore, be sufficient to alter the polymerization of endogenous actin. Because PKCε is not catalytically active in a G-buffer, we believe that this signaling molecule stimulated actin polymerization by a kinase-independent mechanism. These data are consistent with the observations that pharmacological inhibitors of PKC did not impede process formation in 3T3-Lε clones and neurite outgrowth can be induced by expressing a kinase-null regulatory domain fragment of PKCε in neuroblastoma cells [Zeidman et al., 1999]. Even more to the point, the morphological occlusion of 3T3-LΔε clones implies that a hexapeptide motif in the C1 domain of PKCε played a crucial role in the intracellular polymerization of actin and extension of processes by PKCε-transformed fibroblasts. PKCε and F-actin colocalization in these protrusions provided further support for this concept [Prekeris et al., 1998]. The effects of cytochalasin and latrunculin B also made it apparent that actin polymerization was essential for PKCε overproduction to induce process formation in the complex environment of a cell. Finally, PKCε rendered an in vitro pool of thymosin $\beta_4$-sequestered G-actin competent for polymer elongation. This finding suggests that PKCε could potentially be an actin desequestering protein.

PKCε, jasplakinolide, and the profilins are presently the only proteins known to promote actin nucleation and polymer elongation in the presence of a physiologically relevant concentration of thymosin $\beta_4$ (100–600 μM; Pantaloni and Carlier, 1993]. Despite this conspicuous similarity in the in vitro activity of these actin binding proteins, neither profilin nor PKCε are likely to function as an authentic nucleator because the probability of generating new actin trimers or tetramers from a sequestered pool of monomers in vivo is remote [Bailly et al., 1999]. The observation that PKCε effectively binds and stabilizes actin polymers raises the alternative possibility that PKCε generates nucleation activity by stabilizing polymerization intermediates, in a manner that would be reminiscent of the mechanism employed by the Arp2/3 complex for lamellipod extension [Mullins et al., 1998; Bailly et al., 1999]. Such a mechanism of action would be consistent with the observation that PKCε overexpression significantly delayed the collapse of cellular processes following the addition of latrunculin B. The rate limiting step for actin monomer sequestering agents, such as latrunculin B, in filament disassembly would be the rate of subunit dissociation at the pointed end. Thus, by stabilizing actin filament assembly PKCε may have reduced the off-rate of the pointed end and forestalled the actin-disrupting effects of this agent. At the same time, however, free barbed ends must somehow be created for stabile fragments of actin to elongate into filaments at the leading edge of cellular protrusions. In the case of PKCε, this might be accomplished by uncapping barbed ends bound to adducin. Adducins are barbed end actin-capping proteins that are unable to bind actin when their C-terminus has been phosphorylated by PKC [Matsuoka et al., 1998]. Thus, PKCε might promote microfilament assembly by stabilizing short fragments of actin through a direct protein–protein interaction that would be predicted to cooperatively stimulate PKCε activity [Prekeris et al., 1998] and localized uncapping of preexisting barbed ends [Matsuoka et al., 1998]. We remain circumspect toward this hypothesis in the absence of any direct evidence that adducins are recruited to the leading edge of fillopodia, or that uncapping plays a dominant role in generating nucleation sites within this microenvironment [Eddy et al., 1997]. Cofilin provides a plausible alternative mechanism for locally generating free barbed ends in the leading edge of elongate cellular protrusions. This actin severing protein is enriched in the tip of membrane extensions, where it would be capable of generating nucleation sites for polymer elongation [Bailly et al., 1999]. In motile neutrophils, there is now evidence that $Ca^{2+}$-independent isoforms of PKC may indirectly activate cofilin by stimulating the upstream activity of phosphatase 1 and/or 2A [Djafarzadeh and Niggli, 1997]. This would be consistent with our observation that okadaic acid inhibited the formation of cellular extensions in 3T3-Lε-7 cells. Now that there is compelling evidence that PKCε is capable of reshaping a living cell, it seems clear that a detailed analysis of the relationship between PKCε and the generation of free barbed ends within the leading edge of an actively extending fillopodia would be justified.

The major finding of the present study is that the deletion of a small actin binding motif within the C1 domain of PKCε resulted in a clear-cut occlusion of the morphological phenotype established by driving the ectopic expression of PKCε in NIH3T3 fibroblasts. Our results suggest a model, advanced solely to motivate further investigation, wherein PKCε may participate in the generation of protrusive forces required to extend cellular processes by physically interacting with multimeric actin intermediates. This protein–protein interaction may be capable of lowering the critical concentration of actin and, consequently, promoting polymer elongation and process extension in cultured NIH3T3 fibroblasts. Determinants of PKCε-induced changes in cell shape are unknown but are likely to include factors that control the rate of nucleotide exchange on actin monomers, the phosphoinositide cycle, and lipid metabolism. Once active, we predict that PKCε operates as a multifunctional protein to coordinately regulate changes in cell growth and shape. Many important details concerning the complex oncogenic signaling cascade that operates downstream of PKCε remain to be established. However, the potential for PKCε itself to serve as a major effector molecule in the morphological polarization of mesodermal and neuroectodermal cells is now apparent.

## ACKNOWLEDGMENTS

We thank Drs. Rytis Prekeris, Martyn K. White, and James S. deVente for constructing

the mouse p3/PKCε and p5/ΔPKCε $^{222-230}$ cDNAs, Dr. David G. Klapper for providing synthetic peptides, Daniel Whitehead for expert technical assistance on the electron microscope, members of the Dr. Joseph M. Chalovich laboratory for their assistance in preparing pyrenyl-actin, and the members of our laboratory for helpful discussions during the course of these studies

## REFERENCES

Bailly M, Macaluso F, Cammer M, Chan A, Segall JE, Condeelis JS. 1999. Relationship between Arp2/3 complex and the barbed ends of actin filaments at the leading edge of carcinoma cells after epidermal growth factor stimulation. J Cell Biol 331–345.

Cacace AM, Guadagno SN, Krauss RS, Fabbro D, Weinstein IB. 1993. The epsilon isoform of protein kinase C is an oncogene when overexpressed in rat fibroblast. Oncogene 8:2095–2104.

Cacace AM, Ueffing M, Han K–H, Marmè D, Weinstein IB. 1998. Overexpression of PKCε in R6 fibroblasts causes increased production of active TGFβ. J Cell Physiol 175:314–322.

Cooper JA. 1987. Effects of cytochalasin and phalloidin on actin. J Cell Biol 15:1473–1478.

Djafarzadeh S, Niggli V. 1997. Signaling pathways involved in dephosphorylation and localization of the actin-binding protein cofilin in stimulated human neutrophils. Exp Cell Res 236:427–435.

Eddy RJ, Han J, Condeelis JS. 1997. Capping protein terminates but does not initiate chemoattractant-induced actin assembly in Dictyostelium. J Cell Biol 139:1243–1253.

Fagerström S, Påhlman S, Gestblom C, Nånberg E. 1996. Protein kinase Cε is implicated in neurite outgrowth in differentiating human neuroblastoma cells. Cell Growth-Differ 7:775–785.

Genot EM, Parker PJ, Cantrell DA. 1995. Analysis of the role of protein kinase C-α, -ε, and -ζ in T cell activation. J Biol Chem 270:9833–9839.

Gubina E, Rinaudo MS, Szallasi Z, Blumberg PM, Mufson RA. 1998. Overexpression of protein kinase C isoform ϵ but not ( in human interleukin-3-dependent cells suppresses apoptosis and induces bcl-2 expression. Blood 91:823–829.

Hundle B, McMahon T, Dadgar J, Messing RO. 1995. Overexpression of ϵ-protein kinase C enhances nerve growth factor-induced phosphorylation of mitogen-activated protein kinases and neurite outgrowth. J Biol Chem 270:30134–30140.

Knauf JA, Elisei R, Mochly-Rosen D, Liron T, Chen XN, Gonsky R, Korenberg JR, Fagin JA. 1999. Involvement of protein kinase Cepsilon (PKCepsilon) in thyroid cell death. A truncated chimeric PKCepsilon cloned from a thyroid cancer cell line protects thyroid cells from apoptosis. J Biol Chem 274:23414–23425.

Kouyama T, Mihashi K. 1981. Fluorimetry study of N-(1-pyrenyl)iodoacetamide-labelled F-actin. Local structural change of actin protomer both on polymerization and on binding of heavy meromyosin. Eur J Biochem 114:33–38.

Lavie Y, Zhang Z, Cao H, Han T, Jones RC, Liu Y, Jarman M, Hardcastle IR, Giuliano AE, Cabot MC. 1998. Tamoxifen induces selective membrane association of protein kinase C epsilon in MCF-7 human breast cancer cells. Int J Cancer 77:928–932.

Le Good JA, Ziegler WH, Parekh DB, Alessi DR, Cohen P, Parker PJ. 1998. Protein kinase C isotypes controlled by phosphoinositide 3-kinase though the protein kinase PDK1. Science 281:2042–2045.

Matsuoka Y, Li X, Bennett V. 1998. Adducin is an in vivo substrate for protein kinase C: phosphorylation in the MARCKS-related domain inhibits activity in promoting spectrin-actin complexes and occurs in many cells, including dendritic spines of neurons. J Cell Biol 142:485–497.

Mischak H, Goodnight J, Kolch W, Martiny-Baron G, Schaechtle C, Kazanietz MG, Blumberg PM, Pierce JH, Mushinski JF. 1993. Overexpression of protein kinase C-( and -ϵ in NIH3T3 cells induces opposite effects on growth, morphology, anchorage dependence, and tumorigenicity. J Biol Chem 268:6090–6096.

Moriya S, Kazlauskas A, Akimoto K, Hirai S, Mizuno K, Takenawa T, Fukui Y, Watanabe Y, Ozaki S, Ohno S. 1996. Platelet-derived growth factor activates protein kinase Cϵ through redundant and independent signaling pathways involving phospholipase Cγ or phophatidylinositol 3-kinase. Proc Natl Acad Sci USA 93:151–155.

Mullins RD, Heuser JA, Pollard TD. 1998. The interaction of Arp2/3 complex with actin: nucleation, high affinity pointed end capping, and formation of branching networks of filaments. Proc Natl Acad Sci USA 95:6181–6186.

Ohno S, Mizuno K, Adachi Y, Hata A, Akita Y, Akimoto K, Osada S, Hirai S, Suzuki K. 1994. Activation of novel protein kinases C( and Cϵ upon mitogenic stimulation of quiescent rat 3Y1 fibroblasts. J Biol Chem 269:17495–17501.

Pantaloni D, Carlier M. 1993. How profilin promotes actin filament assembly in the presence of thymosin β4. Cell 75:1007–1014.

Perletti GP, Folini M, Lin H, Mischak H, Piccinini F, Tashjian AH Jr. 1996a. Overexpression of protein kinase C epsilon is oncogenic in rat colonic epithelial cells. Oncogene 12:847–854.

Perletti G, Tessitore L, Sesca E, Pani P, Dianzani MU, Piccinini F. 1996b. εPKC acts like a marker of progressive malignancy in rat liver, but fails to enhance tumorigenesis in rat hepatoma cells in culture. Biochem Biophys Res Commun 221:688–691.

Prekeris R, Mayhew MW, Cooper BJ, Terrian DM. 1996. Identification and localization of an actin-binding motif that is unique to the epsilon isoform of protein kinase C and participates in the regulation of synaptic function. J Cell Biol 132:1–14.

Prekeris R, Hernandez RM, Mayhew MW, White MK, Terrian DM. 1998. Molecular analysis of the interactions between protein kinase C-ϵ and filamentous actin. J Biol Chem 273:26790–26798.

Reifel-Miller AE, Conarty DM, Valasek KM, Iversen PW, Burns DJ, Birch KA. 1996. Protein kinase C isozymes differentially regulate promoters containing PEA-3/12-O-tetradecanoylphorbol-13-acetate response element motifs. J Biol Chem 271:21666–21671.

Rybakova IN, Amann KJ, Ervasti JM. 1996. A new model for the interaction of dystrophin with F-actin. J Cell Biol 135:661–672.

Safer D. 1989. An electrophoretic procedure for detecting proteins that bind actin monomers. Anal Biochem 178: 32–37.

Sharif T, Sharif M. 1999. Overexpression of protein kinase C-ϵ in astroglial brain tumor derived cell lines and primary tumor samples. Int J Oncol 15:237–243.

Soh J, Lee EH, Prywes R, Weinstein IB. 1999. Novel roles of specific isoforms of protein kinase C in activation of the c-*fos* serum response element. Mol Cell Biol 19:1313–1324.

Ueffing M, Lovric J, Philipp A, Mischak H, Kolch W. 1997. Protein kinase C-ϵ associates with the Raf-1 kinase and induces the production of growth factors that stimulate Raf-1 activity. Oncogene 15:2921–2927.

Zeidman R, Löfgren B, Påhlman S, Larsson C. 1999. PKCϵ, via its regulatory domain and independently of its catalytic domain, induces neurite-like processes in neuroblastoma cells. J Cell Biol 145:713–726.